TECHNICAL UNIVERSITY OF CIVIL ENGINEERING BUCHAREST

STUDY OF CONDENSATION PHENOMENA ON FLAT SURFACES

Ilie Viorel

Report 1

CUPRINS

INTRODUCTION

The phenomenon of condensation of a fluid (gaseous) on solid surfaces is associated with the heat and mass transfer mechanisms that interfere within the fluid flow in many fields and engineering applications and play an important role in solving two major challenges of the current century: Energy consumption and environmental preservation.

Studies of heat transfer phenomena can be divided into two categories. The first category represent the studies dedicated to the industrial field (nuclear industry, aerospace) where it was intended to increase the amount of energy a surface can receive or give to the outside environment. In addition to the heat transfer, the mass transfer study has become indispensable in such applications. Moreover, it has subsequently been shown that not only mass transfer influences the thermal flux, but also the mechanisms and phenomena associated with mass transfer have an influence that should be taken into account.

The main objective of the second direction is to study the influences that mass transfer has on the movement of the studied fluid, but more important is its influence on the heat transfer. Regarding this matter, an interesting subject is represented by the studies that have as main object the aeraulic analysis inside the rooms or near the solid frontiers. Airflow associated with heat and mass transfer is essential for creating and optimizing energy-efficient systems according to the requirements of the standards.

In the field of building thermotechnics and building installations, the importance of studying the condensation phenomenon grew with the increasingly demanding requirements of air quality standards and energy saving requirments. The main cause of condensation is due to the difficulty of getting a good indoor air humidity control with minimal energy consumption while maintaining the indoor air quality parameters.

The presence of condensation on or inside building elements can lead to early degradation of buildings, but a first negative effect is the quality of indoor air that increases the risk of bacteria. These effects have been noticed during the use of various heating systems. To combat them in the 1950s and 1980s, the use of radiant cooling systems was avoided and all the "attention" turned on air-only systems. Practically, vapor condensation took place on the surface of the cooling coil of the air conditioning system, so the humidity of the air introduced into the air-conditioned space was reduced. This trend has not been maintained because of its negative aspects. One of them is the sensation of thermal discomfort given to the occupants due to the presence of cold airflows. The second incidence was the increased consumption of energy due to the transport of large airflows, but also due to the energy absorbed by the water vapor when changing the phase. In other words, the old problems (degradation of building elements and indoor air quality) have been resolved due to condensation in the undesirable areas of buildings at a much higher price: occupant discomfort and increased energy consumption.

In the early 1980s, technological advances allowed indoor humidity control so the radiative cooling systems began to draw the attention of engineers in the field again by imposing temperatures on cooled surfaces above dew point temperature. This left only the problem of getting the lowest possible energy consumption. In order to achieve this goal, both numerical and experimental studies were carried out. However, due to the complexity of the building geometry, the high construction cost, and due to numerous random factors (building exploitation, variation of indoor humidity and heat sources, climatic conditions), experimental studies proved to be expensive.

In addition, the results obtained in the numerical models for studying heat and mass transfer as well as associated phenomena (surface tension, absorption, desorption) became indispensable in analysis of the phenomena encountered indoor. At the same time, the diversity of phenomena has created the need to divide the analyzes into two categories: vapor transport in the computing field and the evolution of the condensate quantity on the chilled surfaces. This classification also allowed optimization of numerical models inorder to reduce computing time. For example, to analyze indoor air quality in terms of humidity and occupant thermal comfort, it is absolutely necessary to use a numerical model to capture and develop the condensate layer on the studied surface. A first argument would be the fact that for a hygienic and sanitary room, but also for the protection of the building, a number of conditions are required to eliminate the possibility of condensation on surfaces.

To study the physical phenomena mentioned above, the following categories of numerical models can be used: monozone models, multi-zone models, zonal models and CFD (Computational Fluid Dynamics) models.

In this way, it is enough to define mass and energy source terms and then addedto be added to the mass conservation equation of the energy balance equation in the CFD models. The result of this process allows the determination of the speed, temperature and moisture values in any point of the computing domain [Teo.2015]. In addition to these conditions, as mentioned above, the problem of obtaining a low energy consumption is also needed. Regarding this matter, numerical models "evolved" to identify areas with a high risk of condensation ([Liu.2003], [Hoh.2003], [Lon.2005]) in order to impose new boundary conditions (Higher wall temperatures, increased ventilation flow, or recirculated / fresh air drying), so condensation phenomena may be avoided on the internal surfaces of walls with minimum energy consumption. On the other hand, numerical models built for industrial applications (automobiles, aeronautics, mass and heat transfer processes) have been developed in advance of those in the residential sector due to economic factors.

Multi-phase CFD models have often been adopted in numerical models. A good example would be the model presented by [Chi.1998] which uses the boundary layer equations for condensation in the form of a film of steam vapor on a surface in the presence of noncondensable gases. Under different conditions (mixed, free and forced convection), the authors have shown that inertial forces play an important role for reduced Prandtl numbers of fluid. Other multi-phase CFD models have been adopted for possible applications in the nuclear industry ([Drz.2012], [Yad], [Yiz.2011], [Fra.2008]) aeronautical industry ([Kar.2012], [Spa.1999]), chemical industry [Dja.2013], but also in convective flow analysis to improve heat transfer coefficients ([Moh.2007], [Sha.2014]).

The desire to build increasingly competitive systems has developed numerical models that capture as many phenomena as possible regarding the technological process that is studied. Although, a considerable interest remains the analysis of the condensation flow on vertical surfaces. However, if we focus on building thermotechnics, literature offers very few studies using CFD models in simultaneous analysis of both flows. Moreover, they only cover buildings characterized by free water surfaces such as covered swimming pools or baths.

In conclusion, the aim of this paper is to take theoretical elements from the basic scientific literature and which can be used for the development of numerical models for the study of the condensation phenomenon associated with the mass and heat transfer mechanisms encountered inside buildings.

2 THEORETICAL MODELS OF VAPOUR CONDENSATION

When the temperature of the fluid drops below the dew point temperature (characteristic of the studied fluid) we the phenomenon of phase change occurs (condensation). Circumstances in which this phenomena occurs are diverse and their treatment is not the objective of this chapter. The goal is to show how the application of basic principles and simplifying hypotheses can lead to solving mass transfer problems. The starting point around which the entire solution of Bejan's problem is built [Bej.2013] consists in analyzing a simple configuration of condensation flow on a vertical surface taking into account observations that can be made with the naked eye. Thus, through this analysis, it is desirable to assess heat and mass transfer between fluid and wall.

2.1 Laminar film on vertical surfaces

A simple configuration for a phase change situation may be vapor condensation on a vertical cold surface (Fig.2.1). The condensation layer formed on the cooled surface may have three distinct regions. A laminar region at the top of the surface where we encounter a thin coat of condensation. As we move toward to the bottom of the surface, the condensate layer becomes thicker due to the condensing fluid on the surface of the already existing condensate film. Thus, we can distinguish a region where the condensation film becomes thick enough to develop a transient flow regime with Reynolds numbers around 100. In this region the visible surface of the condensate film exhibits small uniform corrugations. If the wall expands sufficiently, the flow of condensation on the surface becomes turbulent and the visible surface of the condensation film will show waves.

On the right side of figure 2.1 we can see that even in the case of laminar flow the fluid flow interacts with the downward boundary layer of the cold vapor flow. The temperature at the liquid-vapor interface is the saturation temperature that corresponds to the local pressure near the wall, Tsat. In this situation we can say that the saturation temperature can be understood as an intermediate temperature that links the vapor temperature of the tank to the wall temperature. Thus, the flow of the condensation film will cause a layer of air that will have a higher temperature than the cold wall but lower than the vapor temperature in the tank.

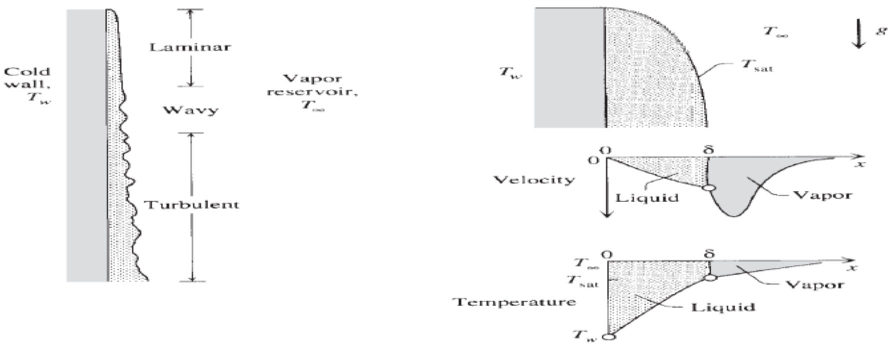

Figura 2.1. Flow patterns of a condensation film on a vertical surface (Bej.2013)

When the flow regime passes from the laminar to the transient and then becomes turbulent, the situation becomes complicated in terms of heat transfer and implicitly the amount of vapor that condenses on the cooled wall. Both heat and mass transfer will increase as the condensation film increase its turbulence level.

Let us consider the laminar condensate represented in Figure 2.1 in which the distance y measures the length of the condensate layer. This representation is a simpler version shown in Figure 2.1 because in this case the fluid in the isothermal tank is considered to be the Tsat saturation pressure. The main advantage of this hypothesis is that it allows neglecting the movement of vapors from the tank and giving full attention to the condensation flow.

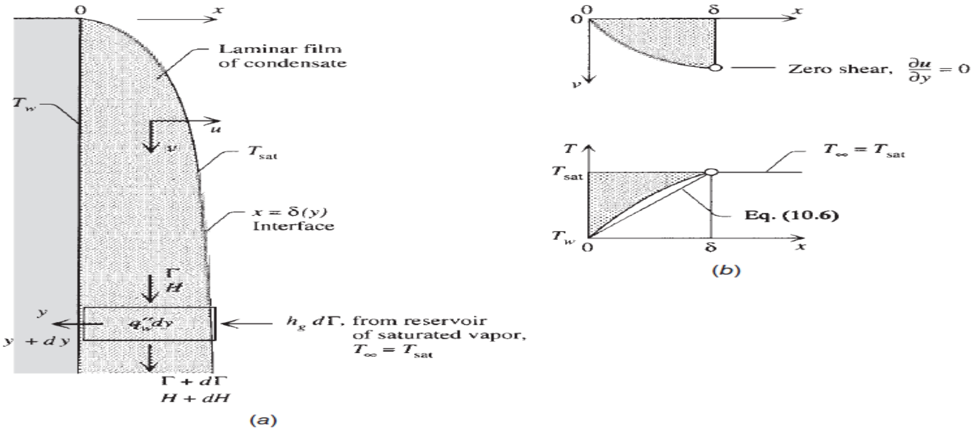

Figura 2.2. Laminar condensation film from a saturated vapor tank [Bej.2013]

Liquid flow analysis begins with the stationary continuity equations, which in the case is reduced to a single equation:

$$\rho_l \left(u \frac{\partial v}{\partial x} + v \frac{\partial v}{\partial y} \right) = -\frac{dP}{dy} + \mu_l \frac{\partial^2 v}{\partial x^2} + \rho_l g \qquad (2.1)$$

The last term on the right is the mass force exerted on each fluid particle. Due to the low thickness of the condensate layer, the pressure gradient inside the liquid is equal to the gradient of the hydrostatic vapor pressure in the tank. DP / dy = ρ_v g. Equation 2.1 can be rewritten by showing that gravitational force acting on the liquid opposes a combination of forces due to friction and inertia:

$$\rho_l \left(u \frac{\partial v}{\partial x} + v \frac{\partial v}{\partial y} \right) = \mu_l \frac{\partial^2 v}{\partial x^2} + g(\rho_l - \rho_v) \qquad (2.2)$$

Where on the left side of the equation we have only one inertial term and on the right we have a first term due to the friction forces and the second due to the gravitational forces.

The analysis continues assuming that the effect of inertia is small compared to the effect due to the friction forces and we can equalize the right part of equation (2.2) with zero.. Without the inertial term, Equation 2.2 can be integrated twice by x and the wall velocity can be considered zero when the variable x is zero (v = 0 at x = 0). In addition, we will consider that shear will be equal to zero at the liquid-vapor interface (∂v / ∂x = 0 for x = δ). The solution for the vertical velocity profile of the liquid is given by the equation:

$$v_{(x,y)} = \frac{g}{\mu_l} (\rho_l - \rho_v) \delta^2 \left[\frac{x}{\delta} - \frac{1}{2} \left(\frac{x}{\delta} \right)^2 \right] \qquad (2.3)$$

Where the thickness of the film is an unknown function that depends on the longitudinal position, δ (y). The mass flow through a cross-section of the condensation film is:

$$\boldsymbol{\Gamma}_{(y)} = \int_0^\delta \boldsymbol{\rho_l v dx} = \frac{g\rho_l}{3\mu_l}(\boldsymbol{\rho_l - \rho_v})\boldsymbol{\delta^3} \quad (2.4)$$

Mass flow C (kg / s * m) is expressed per unit of length in the normal direction to the plane in Figure 2.2. Vertical mass velocity and flow are proportional to the effect given by gravitational forces: g (ρ_l-ρ_v);

The thickness of the condensation film δ (y) can be determined by considering the first law of thermodynamics for the control volume δ x dy presented at the bottom of figure 2.2a. Notice that on the right side of the control volume we have a saturated vapor stream whose enthalpy is $\boldsymbol{h_g d\Gamma}$. The enthalpy associated with the vertical mass flow C (W / m) is:

$$\boldsymbol{H} = \int_0^\delta \boldsymbol{\rho_l v[h_f - c_{P,l}(T_{sat} - T)]dx} \quad (2.5)$$

The term bounded by square brackets is the specific enthalpy (kj / kg) of the fluid at the coordinate point (x, y). Since the liquid experience a slight cooling (T <Tsat), its specific enthalpy will be less than the specific enthalpy of the saturated h_f liquid. We further consider that the local temperature T is distributed approximately linearly along the condensate film [NUS.1916]: $\frac{T_{sat}-T}{T_{sat}-T_w} \sim \mathbf{1} - \frac{x}{\delta}$ (2.6)

Using equations (2.3) and (2.6) in the integral (2.5) we obtain:

$$\boldsymbol{H = [h_f - \tfrac{3}{8} c_{P,l}(T_{sat} - T_w)]\Gamma} \quad (2.7)$$

Returning to the assumption of the linear temperature profile (2.6), the heat absorbed by the wall is:

$$\boldsymbol{q_w^{"} \sim k_l \frac{T_{sat}-T_w}{\delta}} \quad (2.8)$$

The first law of thermodynamics for the system δ x dy imposes the following condition in the stationary regime:

$$\boldsymbol{0 = H - (h + dH) + h_g d\Gamma - q_w^{"} dy} \quad (2.9)$$

Or using equations (2.7) and (2.8):

$$\boldsymbol{\frac{k_l}{\delta}(T_{sat} - T_w)dy = [h_{fg} + \tfrac{3}{8} c_{P,l}(T_{sat} - T_w)]d\Gamma} \quad (2.10)$$

We can assum that the term in the square brackets is a latent condensation heat that also includes the sensible component responsible for condensation cooling at temperatures lower than the Tsat condensation temperature. By combining this term with the expression Γ equation (2.4) and equation (2.10) becomes:

$$\boldsymbol{\frac{k_l v_l (T_{sat}-T_w)}{h'_{fg} g(\rho_l-\rho_v)} dy = \delta^3 d\delta} \quad (2.11)$$

And by integrating from y = 0 where δ = 0,

$$\boldsymbol{\delta}_{(y)} = \left[\boldsymbol{y} \frac{4k_l v_l (T_{sat} - T_w)}{h'_{fg} g (\rho_l - \rho_v)} \right]^{1/4} \tag{2.12}$$

In conclusion, the thickness of the laminar film increases in proportion to its length at the strength ¼. Knowing $\boldsymbol{\delta}_{(y)}$, we can calculate the local heat transfer coefficient:

$$\boldsymbol{h_y} = \frac{q''_w}{T_{sat} - T_w} = \frac{k_l}{\delta} = \left[\frac{k_l^3 h'_{fg} g (\rho_l - \rho_v)}{4 y v_l (T_{sat} - T_w)} \right]^{1/4} \tag{2.13}$$

Average heat transfer coefficient for a L:

$$\overline{\boldsymbol{h_L}} = \frac{4}{3} \boldsymbol{h_{y=L}} \tag{2.14}$$

And the average Nusselt number based on a heat transfer coefficient averaged over a length L:

$$\overline{\boldsymbol{Nu_L}} = \frac{\overline{h_L} L}{k_l} = \mathbf{0.943} \left[\frac{L^3 h'_{fg} g (\rho_l - \rho_v)}{k_l v_l (T_{sat} - T_w)} \right]^{1/4} \tag{2.15}$$

It can be seen that the non-dimensional right-hand term of equation (2.15) is almost equal to the geometric ratio between the length and thickness of the condensation layer:

$$\frac{L}{\delta_{(L)}} = \mathbf{0.943} \left[\frac{L^3 h'_{fg} g (\rho_l - \rho_v)}{k_l v_l (T_{sat} - T_w)} \right]^{1/4} \tag{2.16}$$

In numerical calculations with these formulas, the properties of the liquid are best evaluated for an average condensate film temperature equal to $(T_w+T_{sat})/2$. Latent condensation heat h_{fg} can be found in thermodynamic saturation tables and its value corresponds to the phase shift temperature Tsat. Rohsenow [Roh.1956] refined the previous analysis by eliminating the linear profile hypothesis and integrating the temperature distribution across the film. He found a temperature profile whose curve increases with the degree of cooling of the liquid, $\boldsymbol{c_{p,l}} = (\boldsymbol{T_{sat}} - \boldsymbol{T_w})$. Instead of changing the latent heat $\boldsymbol{h'_{fg}}$ defined by equation (2.10), Rohsenow recommended:

$$\boldsymbol{h'_{fg}} = \boldsymbol{h_{fg}} + \mathbf{0.68} \boldsymbol{c_{p,l}} (\boldsymbol{T_{sat}} - \boldsymbol{T_w}) \tag{2.17}$$

Expression is also recommended for calculations involving both the transient regime and the turbulent flow regime of the condensate film. It can be rewritten in the following form:

$$\boldsymbol{h'_{fg}} = \boldsymbol{h_{fg}} (\mathbf{1} + \mathbf{0.68} \boldsymbol{Ja}) \tag{2.18}$$

Where the Jakob Ja number is a relative measure of the degree of subcooling supported by the liquid film,

$$\boldsymbol{Ja} = \frac{c_{p,l} (T_{sat} - T_w)}{h_{fg}} \tag{2.19}$$

The total heat transfer absorbed by the wall per unit of length in the normal direction to the plane presented in Figure 2.2 is:

$$\boldsymbol{q}' = \overline{\boldsymbol{h}_L}\boldsymbol{L}(\boldsymbol{T}_{sat} - \boldsymbol{T}_w) = \boldsymbol{k}_l(\boldsymbol{T}_{sat} - \boldsymbol{T}_w)\overline{\boldsymbol{Nu}_L} \tag{2.20}$$

The total mass flow collected at the bottom of the wall $\boldsymbol{\Gamma}_{(L)}$ can be calculated by substituting y = L as the result of the combination of equations (2.4) and (2.12). It is easy to show that the total condensation rate $\boldsymbol{\Gamma}_{(L)}$ is proportional to the cooling rate given by the vertical wall,

$$\boldsymbol{\Gamma}_{(L)} = \frac{\boldsymbol{q}'}{\boldsymbol{h}'_{fg}} = \frac{\boldsymbol{k}_l}{\boldsymbol{h}'_{fg}}(\boldsymbol{T}_{sat} - \boldsymbol{T}_w)\overline{\boldsymbol{Nu}_L} \tag{2.21}$$

Equations (2.20) and (2.21) are global and valid for the entire condensation film not only for the laminar section. Rewritten as a form $\boldsymbol{q}' = \boldsymbol{\Gamma}_{(L)}\boldsymbol{h}_{fg}(\mathbf{1} + \mathbf{0.68}\boldsymbol{Ja})$, Equation (2.21) shows that the cooling rate $\boldsymbol{q}'$ increases with the latent heat $\boldsymbol{h}_{fg}$ and the degree of subcoat of the liquid Ja. This tendency is to be expected as the cooling caused by the wall determines

condensation of vapors at the distance x = δ but also cooling of the newly formed liquid at temperatures lower than the T_{sat} saturation. Laminar film resulting from previous Nusselt-derived discussions [Nus.1916] take into account the assumption that the effects of inertia are negligible in the moment equation (2.2). The momentum in the complete form was used by Sparrow and Gregg [Spar.1959] in a similar formulation of the same problem. Their solution for $\overline{\boldsymbol{Nu}_L}$ has a lower value than that given by equation (2.15) when the Prandtl number is less than 0.03 and the Jakob number is greater than 0.01.

In a similar analysis, Chen [Che. 1961] renounced the idea of neglecting the relative movement between liquid and vapor (Figure 2.2), while retaining the effect of inertia in the moment equation. Saturated fumes were considered stationary up to a sufficiently large distance from the interface. Near the liquid vapor interface they are pulled down by the formed liquid stream and form a boundary condition that links the velocity of the condensation film to the stationary vapor inside the tank (see Figure 2.3). Chen's graph for calculating the global Nusselt number is reproduced in Figure 2.4, especially for low Prandtl numbers the values of the $\overline{\boldsymbol{Nu}_L}$ in Figure 2.4 are lower than those in the solution provided by Sparrow and Gregg's [Spa.1959a] but closer to experimental data.

In the dimensional analysis of the Bejan condensation laminar film [Bej 1984], it was shown that the motion of the condensation film is limited by friction when $Pr_l >$ Ja and inertia when Pr_l <Ja. The group that marks the transition from one flow to another is the Pr_l / Ja ratio. Indeed, if we use the Pr_l / Ja ratio on the abscissa of Figure 2.4, the information for the reduced Prandtl numbers in Figure 2.3 is correlated with the curve contained and shown in Figure 2.2:

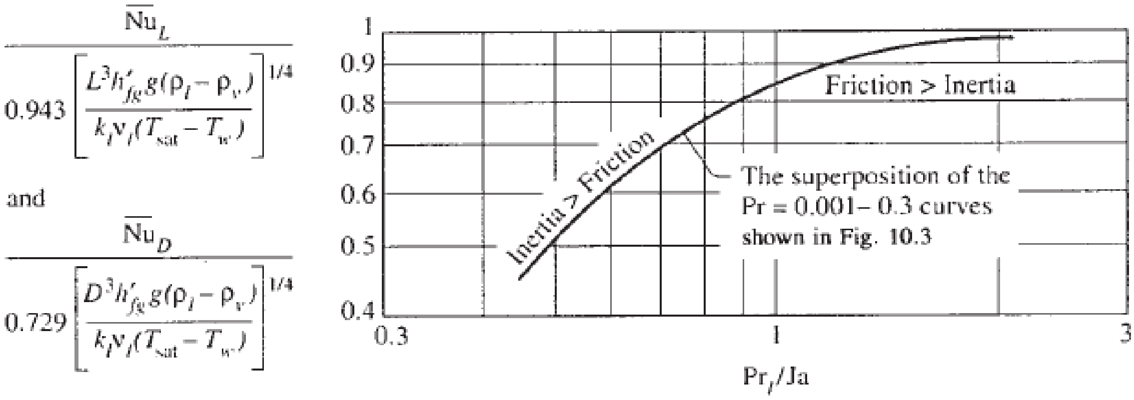

Figura 2.3. The Prandtl number and the effects of subcooling (Ja) on the laminar condensate film on a vertical wall surface and on a horizontal surface of the cylinder ([Bej.1984] and [Che.1961])

Figura 2.4. The transition, from inertial boundaries to friction imposed, condensation of a laminar condensation on a vertical wall and a horizontal cylindrical surface ([Bej.1984] and [Che.1961]

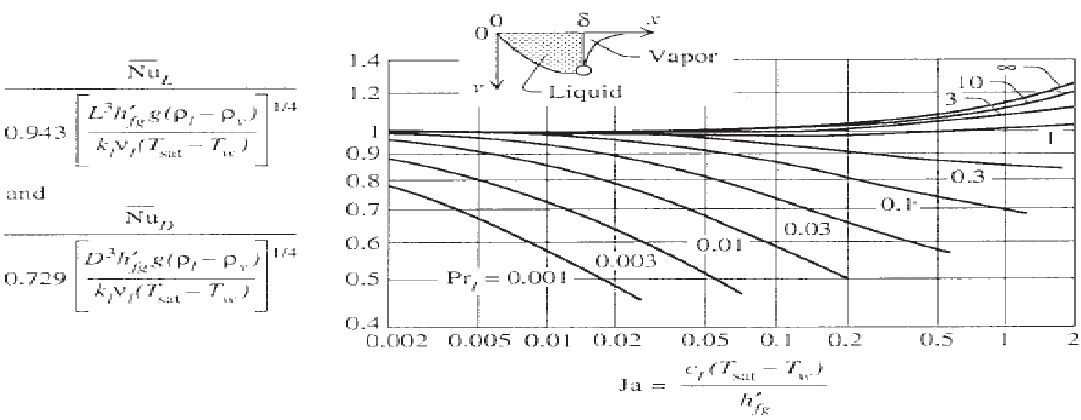

2.2 Turbulent film on vertical surfaces

For high Reynolds flow rates, the surface of the air-to-air condensation film is no longer smooth, and the flow regime passes from laminar to transient and then turbulent. The local Reynolds number of the condensation film is the group $\boldsymbol{\rho_l \bar{u} \delta / \mu_l}$[Bej.1993] where δ represent the thickness and $\boldsymbol{\bar{u}}$ the scale of descending vertical speeds. Because the product $\boldsymbol{\rho_l \bar{u} \delta}$ has the same order of magnitude as the mass flow rate $\boldsymbol{\Gamma}$, the local Reynolds number can also be written in the form $\boldsymbol{\Gamma/\mu_l}$. For this reason, in the field of heat transfer condensation, the local Reynolds number of the liquid film is known in the form,

$$\boldsymbol{Re_y = \frac{4}{\mu_l}\Gamma_{(y)}} \tag{2.22}$$

The mass flow rate $\boldsymbol{\Gamma_{(y)}}$ and the Reynolds number Re_y, increases in the direction of condensation flow. Experimental observations of condensation indicate a disappearance of the laminar film for Re ~ 30. The transient regime is characterized by a Reynolds number whose values fall within the range (30, 1800). The less we move down the film becomes turbulent. The sequence of flows presented can be seen in Figure 2.5.

The experimental data also showed that the heat transfer in the transient and turbulent flow regime has a higher value than in the case of a laminar flow (equation 2.15 and figure 2.3). An experimental analysis containing correlations between heat transfer and flow regime was made by Chen [Che. 1987], which developed the following correlation between the average heat transfer coefficient for a L-height film that may have regions with transient and turbulent:

$$\boldsymbol{\frac{\overline{h_L}}{k_l}\left(\frac{v_l^2}{g}\right)^{1/3} = \left(Re_L^{-0.44} + 5.82 * 10^{-6} Re_L^{0.8} Pr_l^{1.3}\right)^{1/2}} \tag{2.23}$$

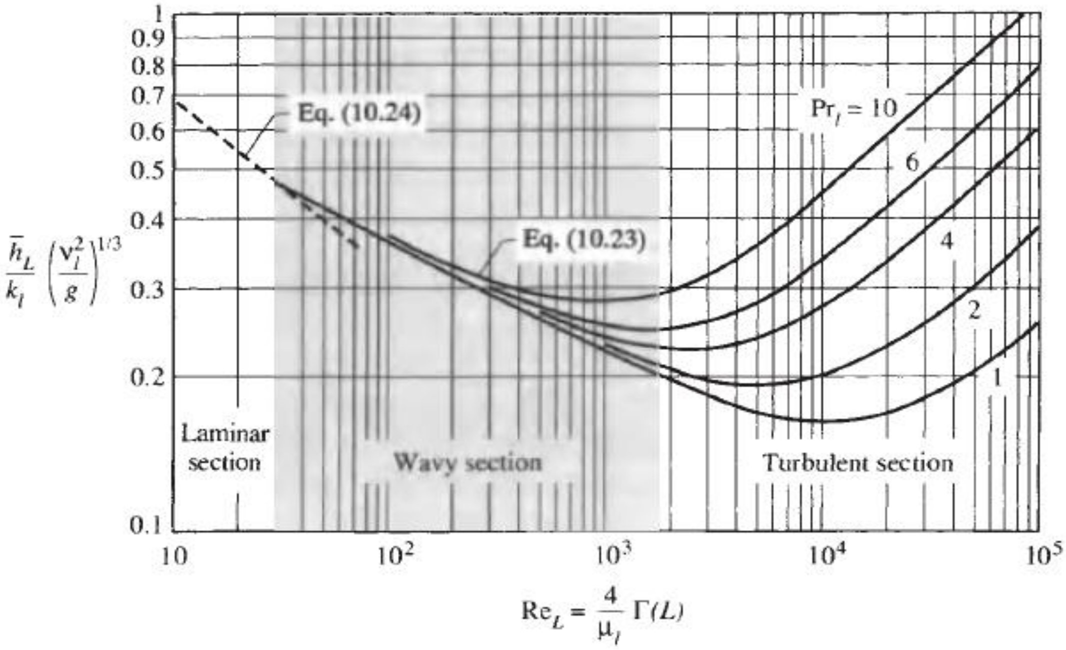

Figura 2.5. The heat transfer coefficient for the laminar, transient and turbulent flow regime for a condensation film on a vertical surface ([Bej.2013]).

According to Figure 2.5, the correlation mentioned above is valid for Reynolds numbers greater than 30. Equation (2.23) gives results similar with experimental data where the shear effect between the condensate and the vapor is negligible. For Reynolds values less than 30, the recommended formula for the mean heat transfer is given by equation (2.15), which, when we impose the condition $\boldsymbol{\rho_l \gg \rho_v}$ can be represented in Figure 2.5 as:

$$\frac{\overline{h_L}}{k_l}\left(\frac{v_l^2}{g}\right)^{1/3} = 1.468Re_L^{-1/3} \qquad (2.24)$$

The main variable in the vertical condensate film analysis is the total condensation rate $\boldsymbol{\Gamma_{(L)}}$, or alternatively, $\mathrm{Re_L}$. This unknown influences present on both sides of the equation (2.23) can be seen in Figure 2.5. Instead of the procedure to try and then calculate the error obtained to solve equation (2.23) or Figure 2.5, it is more convenient to override the ordering parameter in Figure 2.5 as [Bej 1984]:

$$\frac{\overline{h_L}}{k_l}\left(\frac{v_l^2}{g}\right)^{1/3} = \frac{Re_y}{B} \qquad (2.25)$$

Where B is a new dimensional group proportional to the physical quantities L and (T_{sat}-T_w) which, when they grow, tend to increase the condensation rate:

$$B = L(T_{sat} - T_w)\frac{4k_l}{\mu_l h_{fg}'}\left(\frac{g}{v_l^2}\right)^{1/3} \qquad (2.26)$$

Equation 2.26 is a consequence of global relationships (2.20) and (2.21) and allows us to override equations (2.23) and (2.24):

$$\boldsymbol{B = Re_L\left(Re_L^{-0.44} + 5.82 * 10^{-6} Re_L^{0.8} Pr_l^{1.3}\right)^{-1/2}} \quad (2.27)$$

$$\boldsymbol{B = 0.681 Re_L^{4/3}} \quad (2.28)$$

Figure 2.6 shows this information using Re_L on the abscissa and parameter B on the ordonate. We can also see that the condensation rate increases faster when the turbulent regime is present.

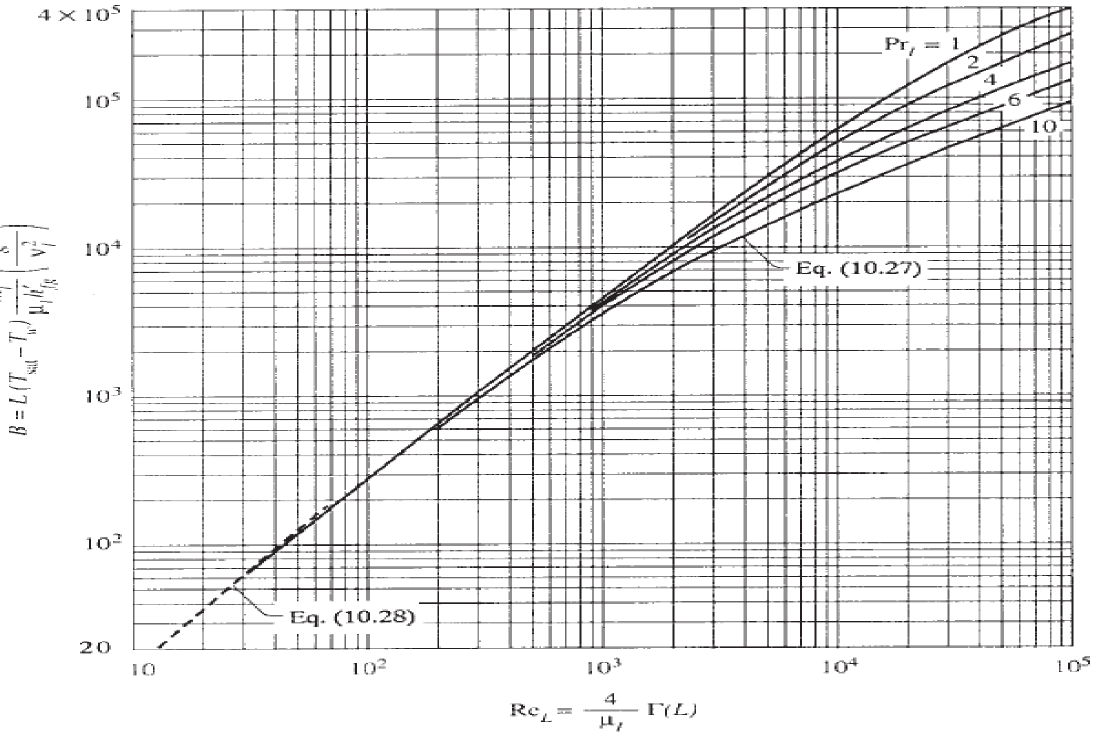

Figura 2.6. Condensing film on a vertical surface: the total condensation rate as a function of the constraint parameter B [Bej.2013].

2.3 Droplet condensation

Experimental studies have shown that the heat and mass transfer rate is much higher when drop condensation happen than the case of condensation in the form of a continuous condensate film for the same conditions [Gar 1966] [Gr.1965].

Several theories have been developed since the last century. The first theory was exposed by Jakob [Jak.1955]. Starting from a simple case: water vapor condensation on a chilled surface. High values of heat transfer coefficients are explained by the fact that in such cases the water vapor comes in direct contact with the cooled surface, forms a continuous vapor layer near the cooled surface, condenses and then forms a thin layer of water on the surface . Over time, the condensate layer becomes thicker, breaks down to form droplets. The formed droplets under the influence of external forces are moved, leaving behind a dry surface which then allows the formation of new droplets. At the same time, there is the possibility that the moving droplets will merge with other smaller droplets in its descending path. Since the condensation rate is maximal in the absence of condensate film on the surface (as a film or droplets), periodic cleaning is performed by droplets that renew finite regions of the surface, thus creating a repetitive condensation process. [Bej.1999].

In comparison with Bejan's analysis (Bej.1993) of a vertical condensate film (Chapter 2), Jakob retains the idea of forming a continuous condensate layer until the moment the thickness increases. Basically, instead of a stable film defined by different flow and variable thickness regimes, we will have a film whose thickness is limited by the superior instability due to the droplet formation mechanism. In other words, if the thickness of Nusselt's condensation film depends on condensation and wall height, Jakob's film, responsible for droplet formation, depends on the purity of water vapor and the properties of the chilled surface.

Even though Jakob's theory has been supported by Welch and Westwater microscopic studies [Wel.1961], application to numerical models represented at 1:1 scale is almost impossible to achieve at present. Practically, the need to create a fine mesh network in order to capture the appearance of Jakob's microfilm leads to an exponential increase in calculation time for any numerical simulations.

Another theory of condensation in the form of droplets was proposed by Emmons [Emm. 1939]. He suggested that the molecular processes of evaporation, condensation and reflection of surface molecules studied in connection with the catalytic emission of electrons can be applied to the condensation mechanism in the form of droplets [Gar.1969]. It defines Nusselt's laminar film as being composed of several layers. The first layer of condensation occurs when the rate of arrival of water vapor molecules is higher than of those leaving the surface. In this way, the vapor molecules will accumulate near the lower temperature limit but before the entire surface is covered, some of the vapor molecules will come above the first layer already fixed to the surface, representing the first elements of the second layer. The process can continue in two ways, depending on the balance between the intermolecular forces inside the liquid and the forces between the liquid and the surface. If the adhesion forces are large enough, the liquid will *wet* the cooled surface by forming a laminar condensate film comprising several layers characterized by different flow rates. If the intermolecular forces predominate, a first layer of condensation will appear on a small portion of the surface, and the appearance of the next layers will lead to the formation of the first droplets of condensate. According to Emmos, droplets only appear when there is a thin layer of supersaturated vapors on the surface. When droplets begin their downward movement they will interact with the saturated vapor layer resulting in a rapid condensation around the droplet. Local pressure is reduced in the droplet area, so local vapor currents are generated around droplets. This explains the mechanism responsible for the high values of heat transfer coefficients

In conclusion to these theories, we can say that for a detailed analysis of the condensation phenomenon it is necessary to determine in advance the form that the water vapor will take from the condensation: film or droplets. The numerical analysis of the condensation phenomenon in the form of droplets is complicated by the temporal composition, the dominant effect of the superficial stress (the shape and size of the condensate droplet) and the uncertainty about the precise position where the condensate droplets will occur, but also the moment when the large droplets will start the downward movement. A theory of condensation in the form of droplets on a surface to come up with solutions to the main problems mentioned above has not yet been fully developed.

In the scientific literature, we can find some numerical models that can represent or provide an idea that can lead to the development of a numerical model that takes into account the effects of condensation in the form of drops on heat and mass transfer. We can recall two representative models that correlate Young's contact angle with the geometric shape of the droplets in contact with the surface: the Wenzel model and the Cassie-Baxter model. Both models define the degree of watering of the surfaces according to their roughness and texture. The main problem is represented by the physical techniques required for the designing of specific roughnesses. But with the technological advancing, methods of modification of the surface roughness advanced and superhidrophobic surfaces were defined. It should be noted that maintaining this superhydrophobicity property is a problem for which solutions are still being sought. Practically due to the external factors determined mainly by the cyclic processes, it causes deterioration of the surface texture and implicitly of the hydrophobicity property.

3 NUMERICAL MODELS APPLIED ON BUIDINGS

3.1 Introduction

The numerical modeling of the condensation phenomenon and the study of the evolution of the condensate on cooled surfaces represented an increased interest in the field of building thermotechnics. The last two decades have been a period of major changes in the design of facilities for dwellings. If in the past we wanted to build as many buildings as possible, nowadays we can not conceive a building without taking into account three criteria: indoor air quality, occupant thermal comfort and energy efficiency. Moreover, these criteria are the basis for the sizing and choice of building facilities. At the same time, indoor air humidity can have negative effects on the occupants as well as on the building [Lon.2005]. Although the negative effects of humidity are well known, a numerical model that treats the coupling between humidity, heat transfer, air flow and analysis of heat transfer coefficient according to the geometric form of condensed vapor on building surfaces is not yet fully developed. However, the number of studies on this direction has seen considerable in progress in recent years ([Teo.2013], [Gon.2011]).

3.2 INTERNATIONAL ENERGY AGENCY PROPOSED MODEL [IEA.1991]

A numerical model that takes into account humidity, air flow and heat transfer can be based on CFD (Computational Fluid Dynamics) technique, adding an equation for preserving the mass fraction of water vapor equations describing the non-isothermal and turbulent flow of humid air. Humid air is considered to be a mixture of dry air and water vapor. The newly added equation can be written in the following form:

$$\rho \frac{\partial}{\partial x_i}\left(u_i m_{i'}\right) + \frac{\partial}{\partial x_i} J_{i',i} = S_{i'} \tag{3.1}$$

Where the terms on the left side of the equation are terms due to convection (ρ - density, x_i - spatial coordinate, u_i - velocity component in the direction i, m_i '- the mass fraction of water vapor) and the terms due to diffusion (J_i, Diffusive water vapor stream). The term on the left side of the equation represent the source terms.

The diffusion term in equation (4.1) contains both the molecular component and the turbulent component. Molecular diffusion is solved by Fick's law (the diffusive flow of water vapor is proportional to the concentration gradient). On the other hand, turbulent water vapor diffusion is solved by the turbulence model chosen to describe humid air flow in the CFD simulation.

Regarding the condensation modeling in buildings, the International Energy Agency proposes a specific model [IEA.1991]. Within this model, the condensate water vapor flow density is calculated considering the transport of water vapor into the air is largely achieved only by convection. On the other hand, near solid walls, diffusion becomes the main component:

$$\Phi_{vap.cond} = \beta(P_{vap.air} - P_{vap.surface}) \tag{3.2}$$

Where β (s / m) is a proportionality coefficient describing the diffusion of water vapor between the inner environment and the surface of the walls, the vapor pressure in the air and the vapor pressure on the surface of the walls. In addition, the coefficient β in equation 4.2 may be correlated with the heat transfer coefficient for applications that include heat transfer in buildings [IEA.1991]. Thus, the coefficient β in equation (4.2) varies with the heat transfer coefficient, resulting from the calculation of heat exchange between fluid and solid surfaces (within CFD simulations).

$$\Phi = h_c(T_w - T_{aer})S = h_c(T_F - T_{C0})S_F \quad (3.3)$$

Where the terms of equation (4.5) have the following meanings: T_w - temperature on the surface of the walls, T_{aer} - ambient temperature, S - surface of a face, T_{co} - temperature in the center of gravity of the cell layer adjacent to the wall (Figure 3.1).

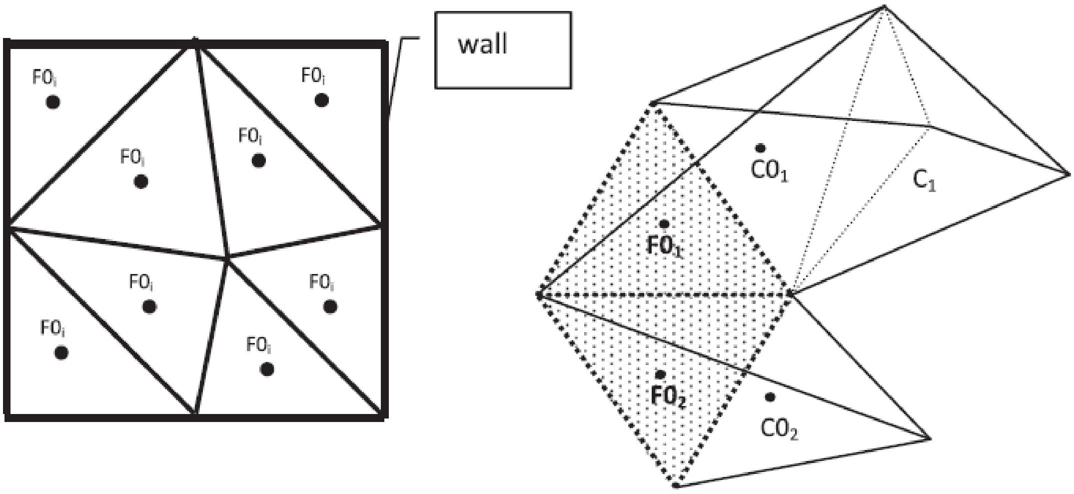

Figura 3.1: Discretizarea stratului limită și a suprafețelor [Teo.2013]

On the other hand, the viscous region near the walls is characterized in terms of heat exchanges due mainly to conduction mechanism. In this case the convection can be neglected. Consequently, the density of the heat flux is taken into account by Fourier's law, so the heat transfer coefficient is determined as follows:

$$\varphi = -\lambda_{air}\,\overrightarrow{grad}T\vec{n} = \lambda_{air}\left(\frac{\partial T}{\partial n}\right) = h_c(T_F - T_{C0}) => h_c = \frac{\lambda_{air}}{(T_F - T_{C0})}\left(\frac{\partial T}{\partial n}\right) \quad \textbf{(3.4)}$$

Where λair - the thermal conductivity of humid air and the temperature gradient is calculated with the following formula:

$$\left(\frac{\partial T}{\partial n}\right) = \frac{(T_F - T_{C0})}{S_F}\alpha \quad (3.5)$$

Where S_F represents the area of a triangle α:

$$\alpha = \frac{\overrightarrow{S_F} * \overrightarrow{S_F}}{\overrightarrow{S_F} * \overrightarrow{s_0}}$$

cu s_0 = (coord$_F$ – coord$_{C0}$).

From equation (3.4), the value of the convective heat transfer coefficient is determined for each cell in the mesh that has a common face with one of the solid areas of the computing domain, taking into account the following data:

- temperature difference between the center of gravity of the common triangular face (mesh cell and solid surface) and the center of gravity of the cell.

- the distance between the triangle and the center of gravity of the triangle-containing cell.

- the thermal conduction of humid air in the center of the cell [Teo.2013].

Once the coefficient has been solved, the mass transfer rate (condensation rate) on the $m_{vap.cond}$ surface is calculated for each cell of the mesh domain having a common face with the solid surfaces [Teo.2013]:

$$\dot{m}_{vap.cond} = \frac{dm_{liq.surface}}{dt} \tag{3.6}$$

if

$$P_{vap} - P_{vap.sat} > 0$$

$$\dot{m}_{liq.surface} = 7,4\text{x}10^{-9} h_c S_{F_i} (P_{vap.} - P_{vap.sat})$$

else

$$\dot{m}_{liq.surface} = 0$$

Where $m_{liq.surface}$ – condensation rate, based on equation (3.2), $p_{vap.sat}$ - the saturation pressure of the water vapor. Pvap- Partial water vapor pressure.

Using the water vapor condensation rate on the surface, the connection to the calculation volume is accomplished by the mass and energy balance equations [Teo.2013].

3.3 EVAPORATION CONDENSATION MODEL

The condensation evaporation model proposed by [Lee.1979] is a model that can be used in CFD models. It's use is closely related to the multiphase term allowing simultaneous analysis of multiple flows. In the case of the humid air and condensation study, besides the definition of the air-water mixture, water is also defined as the secondary phase. The separation between the two phases is performed by means of an interface located at the boundary between the gaseous fluid (wet air) and the condensed water vapor on the chilled surface. Mass transport at the fluid-liquid interface is governed by the following transport equation:

$$\frac{\partial}{\partial t}(\alpha\rho_v) + \nabla\left(\alpha\rho_v\vec{V}_v\right) = \dot{m}_{l\to v} - \dot{m}_{v\to l} \quad (3.7)$$

v – gase state; α – vapor mass fraction; ρ_v – vapor density; $\vec{V}_v$ - vapor velocity; $\dot{m}_{l\to v}, \dot{m}_{v\to l}$ – evaporation and condensation rates;

It is noted that in the water vapor transport equation (3.7) the mass transfer is considered positive when the evaporation process takes place. Depending on the temperature regime, mass transfer can be described as follows:

- if $T_l>T_{sat}$ then $\dot{m}_{l\to v} = coeff * \alpha_l\rho_l \frac{T_l - T_{sat}}{T_{sat}}$ (3.8)
- if $T_v>T_{sat}$ then $\dot{m}_{l\to v} = coeff * \alpha_v\rho_v \frac{T_l - T_{sat}}{T_{sat}}$ (3.9)

Where the term coeff - is a coefficient that can be interpreted as a relaxation factor. The source term for the energy equation can be obtained as the result of the product between the mass transfer rate and the latent heat of the water when changing the phase from liquid to vapor or vapor in the liquid. Considerând formula Hertz Knudsen [Her.1881] [Knu.1915], se poate determina fluxul de evaporare-condensare în funcție de teoria cinetică pentru o interfață plană:

$$F = \beta\sqrt{\frac{M}{2\pi R T_{sat}}}(P^* - P_{sat}) \quad (3.10)$$

Where: F - the flow is expressed in kg / s / m2; P - the pressure; T - temperature; R - universal gas constant;

The coefficient β represents the amount of water vapor molecules that are transferred to and absorbed by the liquid surface. P * represents the partial pressure of water vapor at the gas-liquid interface on the gas side. The Clapeyron-Clausius equation relates pressure and temperature to the saturation condition (obtained by equalizing chemical vapor and liquid potentials):

$$\frac{dP}{dT} = \frac{L}{T(v_g - v_l)} \tag{3.11}$$

v_g si v_l is the volume per unit area of gas and liquid; L - latent vaporization heat (J / kg);

Starting from differential expression, we can get the temperature variation from the variation in pressure close to the saturation condition.

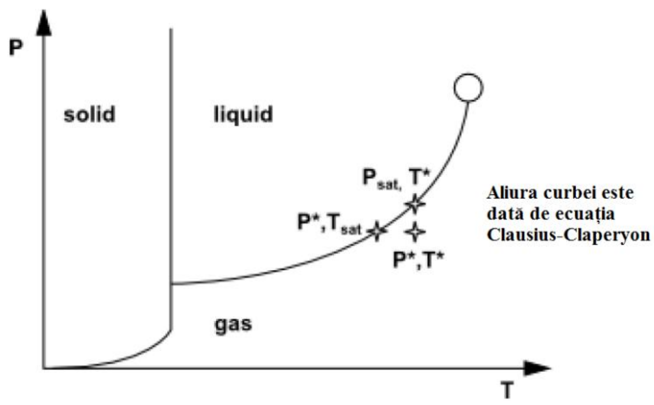

Figura 3.2 Diagrama stabilității fazei [Ans.2013]

The Clausius-Clapeyron equation leads to the following formula as long as P * and T * are close to the saturation condition:

$$P^* - P_{sat} = -\frac{L}{T(v_g - v_{l)}}(T^* - T_{sat}) \tag{3.12}$$

Using this relationship in the Hertz Knudsen equation (3.10) results:

$$F = \beta\sqrt{\frac{M}{2\pi R T_{sat}}} L \left(\frac{\rho_g \rho_l}{\rho_g - \rho_l}\right) \frac{(T^* - T_{sat})}{T_{sat}} \tag{3.13}$$

Factor β is defined by the properties of the fluid (water vapor). It approaches the value 1 near the equilibrium conditions. In flow-specific multiphase models the flow regime is assumed to be dispersed. Assuming that all vapor bubbles have the same diameter then the density of the area is given by the following calculation relation:

$$\frac{A_l}{V_{cel}} = \frac{6a_v}{d} \tag{3.14}$$

The cell represents the cell volume and the phase source phase (kg / s / m3) becomes:

$$F\frac{A_l}{V_{cell}} = \frac{6}{d}\beta\sqrt{\frac{M}{2\pi R T_{sat}}} L \left(\frac{\rho_l}{\rho_l - \rho_g}\right)\left[\rho_g \alpha_v \frac{(T^* - T_{sat})}{T_{sat}}\right] \tag{3.15}$$

From equation (3.15), the **coeff** coefficient is the inverse of the relaxation time (1/s) and can be defined as:

$$coeff = \frac{6}{d}\beta\sqrt{\frac{M}{2\pi R T_{sat}}}L\left(\frac{\rho_l}{\rho_l-\rho_g}\right) \quad (3.16)$$

This relationship leads to the final expression for vaporization of the liquid, as defined by equation (3.9). Similar expression can be obtained for condensation. In this case, the small droplets are considered to be in a continuous phase of water vapor even if the primary phase is a liquid. Note that the **coeff** coefficient, theoretically, should be different for condensation and evaporation expressions.

Moreover, the theoretical expression is based on the following simplifying assumptions:

- Flat interface
- Constant dispersed mode;
- The β coefficient is known;

The main inconvenience is related to the setting of the bubble diameter values and the β coefficient, since in most situations they are not known. For this reason, the coeff coefficient is chosen arbitrarily or according to experimental data available.

4 CONCLUSIONS

In the literature, different theoretical and numerical approaches are proposed for the study of the condensation phenomenon on solid surfaces.

An interesting approach to the condensation layer modeling is to define the boundary layer as a layer adjacent to the condensation film and which is at rest from it. Practically, relative motion between the condensation and vapor film is neglected, obtaining close results from experimental data [Che. 1961]. On the other hand, it has been demonstrated that the motion of the condensation film is directly related to the inertia forces and limited by the friction forces [Bej.2013]. Based on the experimental data taken into account in the models [Bej.1984], [Bej.1993], [Bej.2013] it was shown that the heat transfer rate for the condensation flow on vertical surfaces characterized by transient and turbulent flow regimes record values higher than in the laminar regime. This fact also affects the condensation rate.

The formation of the transient or turbulent flow regime is possible when the height of the wall or the vertical surface allows it. Practically, the mass forces must be greater than the frictional forces and act on the fluid for a long time so that the "kinetic energy" "surplus" can be turned into turbulent energy. It is also noted that the literature is quite generous in the development of film condensation on surfaces([Spa.1959a], [Che. 1961], [Bej.1984], [Bej.1993] [Bej.2013], [Che.1987], [Chi.1998], Mic.09], [Sun.2012]) which led to the creation and development of new numerical models.

On the other hand, the phenomenon of condensation in the form of droplets on chilled surfaces has been studied in industrial applications (eg heat exchangers) and very little in the field of building thermotechnics. Thus, a complete numerical model that translates the physical phenomenon into mathematical equations has not yet been developed.

The problems of mass transfer modeling in this situation are complex because it is not possible to determine precisely the positions, the dimensions and the moment when the first droplets of condensate will appear on the chilled surface. Until now, only experimental studies have been able to provide realistic data for the calibration of certain numerical models. The best example is the [Lee.1979] model where a coefficient need to be set by the user in order to take into account the droplet size and to calculate the condensation or evaporation rate.

Basically, the validity of results depends very much on experimental data for each studied configuration. Another problem whose numerical solution is delayed is to determine the moment when the condensate droplets will begin to descend the vertical wall.

With regard to the condensation patterns in the form of droplets, an important objective is to determine the heat transfer rate. In this respect experimental studies show that the rate of thermal transfer can increase substantially if the condensation occurs as an continous film.

Another important aspect of condensation in the form of droplets is that this mass transfer method does not depend only on the degree of wettability of the surface but also on its morphology. Thus, in the past, dropwise condensation can also be applied in engineering applications for surface self-cleaning (eg the helmet windshield of the pilots' of formula 1). The self-cleaning effect has been studied by analyzing how the leaves of the lotus plant "reject" water droplets ([Bar.1997]).

Based on the review of the models proposed in the literature, it can be concluded that starting from the [IEA.1991] model, a methodology can be developed to simulate the condensation on cold surfaces in the construction field. The model is based on the definition of energy and mass source terms added to the water vapor preservation equation (3.1) for modeling water vapor transport within the computing domain.

REFERENCES

[Ans.2013] ANSYS Fluent Theory Guide ANSYS, Inc. Release 15.0, Southpointe November 2013, 275 Technology Drive, Canonsburg, PA 15317

[Bar.1997] Barthlott, W. & C. Neinhuis (1997): Purity of the sacred lotus, or escape from contamination in biological surfaces. Planta 202: 1-8

[Bej.1984] A. Bejan, Convection Heat Transfer, Wiley, New York, 1983.

[Bej.1993] A. Bejan, Heat Transfer, Wiley, New York, 1993

[Bej.1999] J. V. C. Vargas and A. Bejan, Optimization of film condensation with periodic wall cleaning, Int. J. Thermal Sci., Vol. 38, 1999, pp. 113–120.

[Bej.2006] A. Bejan, Advanced Engineering Thermodynamics, 3rd edition, Wiley, Hoboken, 2006.

[Bej.2013] Adrian Bejan, Convection Heat Transfer, Fourth Edition. 2013 John Wiley & Sons, Inc. Published 2013 by John Wiley & Sons, Inc., 428p.

[Che.1961] M. M. Chen, An analytical study of laminar film condensation: 1. Flat plates, J. Heat Transfer, Vol. 83, 1961, pp. 48–53.

[Che.1987] S. L. Chen, F. M. Gerner, and C. L. Tien, General film condensation correlations, Exp. Heat Transfer, Vol. 1, 1987, pp. 93–107.

[Che.1964a] P. Cheng. "Two-Dimensional Radiating Gas Flow by a Moment Method". AIAA Journal. 2. 1662–1664, 1964.

[Chi.1998] Chin YS, Ormiston SJ, Soliman HM (1998) A two-phase boundary-layer model for laminar mixed convection condensation with a noncondensable gas on inclined plates. Heat Mass Transf 34:271–277

[Chu.1988] G. D. Raithby and E. H. Chui, A Finite-Volume Method for Predicting a Radiant Heat Transfer in Enclosures With Participating Media, J. Heat Transfer 112(2), 415-423 (May 01, 1990) (9 pages), doi:10.1115/1.2910394.

[Cun.2013] Cunjing Lv, Pengfei Hao, Zhaohui Yao, Yu Song, Xiwen Zhang, Feng He, Condensation and jumping relay of droplets on lotus leaf, Department of Engineering Mechanics, Tsinghua University, Beijing 100084, China, submitted 2013, DOI: 10.1063/1.4812976

[Dja.2013] Djamel Lakehal ADVANCED SIMULATION OF TRANSIENT MULTIPHASE FLOW & FLOW ASSURANCE IN THE OIL & GAS INDUSTRY; THE CANADIAN JOURNAL OF CHEMICAL ENGINEERING, VOLUME 9999, 2013

[Drz.2012] Timothy J. Drzewiecki, Isaac M. Asher, Timothy P. Grunloh, Victor E. Petrov, Krzysztof J. Fidkowski, Annalisa Manera and Thomas J. DownarParameter Sensitivity Study of Boiling and Two-Phase Flow Models in CFD;The Journal of Computational Multiphase Flows Volume 4 · Number 4 · 2012

[Edd.1959] Eddington, A. S.: “The Internal Constitution of Stars,” Dover, New York, 1959.

[Emm.1939] Emonsi H., "The Mechanism of Dropwise Condensation," American Institute of Chemical Engineers, Trans., Vol. 35, 1939, pp, 109-125.

[Fra.2008] Th. Frank1, P.J. Zwart2, E. Krepper3, H.-M. Prasser3, D. Lucas3; VALIDATION OF CFD MODELS FOR MONO- AND POLYDISPERSE AIR-WATER TWO-PHASE FLOWS IN PIPES;Nuclear Engineering and Design 238 (2008) 647–659

[Gar.1969] S. C. Garg, “THE EFFECT OF COATINGS AND SURFACES ON DROPWISE CONDENSATION”, Technical Note N-1041, NAVAL CIVIL ENGINEERING LABORATOY Port Hueneme, California 93041, 1969.

[Gon.2013] Guangcai Gong*, Chunwen Xu, Junjun Jiao, Yuankun Liu, Sainan Xie, Investigation of moisture condensation on papermaking plant envelopes in high, humidity environment by orthogonal analysis and CFD simulation, Chemical Engineering Research Center, State Key Laboratory of Chemical Engineering, School of Chemical Engineering and Technology, Tianjin University, Tianjin, 300072, China, Building and Environment Journal 2011.

[Gri.1965] Umur, A. and-Griffith, P., "Mechanism of Dropwise Condensation," Trans. of ASME, Journal of Heat Transfer, Series C, No. 2, 1965, pp. 275-282.

[Her.1882] H. Hertz. “On the Evaporation of Liquids, Especially Mercury, in Vacuo”. Annalen der Physik (Leipzig).17. 177. 1882.

[Hoh.2003] Hohota R., Modelisation de l’humidite dans un code CFD (basses vitesses en grand cavite). Compairasonavec l’experimental. Teza doct.:Institut National des Sciences Appliquees de Lyon, 2003

[IEA.1991] International Energy Agency (IEA). Energy conservation in buildings and community systems programme. IEA – Report Annex 14, vol 1;1991.

[Jak.1955] Jakob, M., “Heat Tansfer in Evaporation and Condensation – II”, Mechanical Engineering, Vol. 58, 1936, pag. 729-739

[JUN.2012] Jun-De Li, CFD simulation of water vapour condensation in the presence of non-condensable gas in vertical cylindrical condensers, International Journal of Heat and Mass Transfer 57 (2013) 708-721

[Kar.2012] S.J. Karabelas ∗, N.C. Markatos Water vapor condensation in forced convection flow over an airfoil, International Journal of Heat and Mass Transfer 55 (2012) 5479–5494

[Knu.1915] M. Knudsen. “Maximum Rate of Vaporization of Mercury”. Annalen der Physik (Leipzig). 47. 697. 1915.

[Kun.1997] Kunal Mitra, Ming-Sing Lai, and Sunil Kumar. "Transient Radiation Transport in Participating Media Within a Rectangular Enclosure", Journal of Thermophysics and Heat Transfer, Vol. 11, No. 3 (1997), pp. 409-414./doi: 10.2514/2.6255

[Lee.1979] W. H. Lee. "A Pressure Iteration Scheme for Two-Phase Modeling". Technical Report LA-UR 79-975. Los Alamos Scientific Laboratory, Los Alamos, New Mexico. 1979

[Liu.2003] Liu Jing, Yoshihiro Aizawa, Hiroshi Yoshino, EXPERIMENTAL AND CFD STUDIES ON SURFACE CONDENSATION; Eighth international IBPSA Conference Eindhoven, Netherlands, August 11-14, 2003;

[Lon.2005] Lone Hedegaard Mortensen, Monika Woloszyn, Raluca Hohota and Gilles Rusaouën; MODELLING OF MOISTURE INTERACTIONS BETWEEN AIR AND CONSTRUCTIONS, Ninth International IBPSA Conference Montréal, Canada August 15-18, 2005;

[Mar.2003] Abraham Marmur (2003). "Wetting of Hydrophobic Rough Surfaces: To be heterogeneous or not to be". Langmuir 19 (20): 8343–8348.

[Mar.2004a] Shigenao Maruyama, , Yusuke Mori, Seigo Sakai, Nongray radiative heat transfer analysis in the anisotropic scattering fog layer subjected to solar irradiation, Journal of Quantitative Spectroscopy and Radiative Transfer, Volume 83, Issues 3–4, 1 February 2004, Pages 361–375.

[Man.2012] H. B. Eral, D. J. C. M. ’t Mannetje, J. M. Oh, Contact angle hysteresis: a review of fundamentals and applications, Colloid and Polymer Science February 2013, Volume 291, Issue 2, pp 247-260 Date: 14 Sep 2012

[Men.2010] Mengnan Qu, Jinmei He and Junyan Zhang (2010). Superhydrophobicity, Learn from the Lotus Leaf, Biomimetics Learning from Nature, Amitava Mukherjee (Ed.), ISBN: 978-953-307-025-4, InTech, DOI: 10.5772/8789. Available from: http://www.intechopen.com/books/biomimetics-learning-from-nature/superhydrophobicity-learn-from-the-lotus-leaf

[Mil.1930] Milne, F. A.: Thermodynamics of the Stars, “Handbuch der Astrophysik.” Vol. 3, pp. 65-255, Springer-Verlag, OHG, Berlin, 1930.

[Mic.2009] Michael Favre-Marinet, Sedat Tardu, Convective Heat transfer Solved Problems, ISTE Ltd and John Wiley&Sons, Inc , 2009.

[Mod.1993] M. F. Modest. Radiative Heat Transfer. Series in Mechanical EngineeringMcGraw-Hill. 1993.

[Moh.2007] A. Belhadj Mohamed, J. Orfi*, C. Debissi, S. Ben Nasrallah Condensation of water vapor in a vertical channel by mixed convection of humid air in the presence of a liquid film flowing down; Desalination 204 (2007) 471–481

[Nus.1916] W. Nusselt, Die Oberfl¨achenkondensation der Wasserdampfes, Z. Ver. Dtsch.Ing.,Vol. 60, 1916, 541p–569p

[Roh.1956] W. M. Rohsenow, Heat transfer and temperature distribution in laminar-film condensation, Trans. ASME, Vol. 78, 1956, pp. 1645–1648.

[Sha.2014] Ali Shahmohammadi, Arezou Jafari, Application of different CFD multiphase models to investigate effects of baffles and nanoparticles on heat transfer enhancement; Chemical engineering Departament, Tarbiat Modares University, Tehran 114-14115, Iran; Higher Education Press and Springer-Verlag Berlin Heidelberg 2014;

[Sig.1992] Robert Siegel, John R. Howell, Thermal Radiation Heat transfer, Third edition, Hemisphere Publishing Corporation (a member of the Taylor & Francis Group) 1992.

[Spa.1999] P.R. Spalart, S.R. Allmaras, A One Equation Turbulence Model for Aerodynamic Flows, AIAA, 1999.

[Spa.1959a] E. M. Sparrow and J. L. Gregg, A boundary-layer treatment of laminar-film condensation, J. Heat Transfer, Vol. 81, 1959, pp. 13–18

[Spa.1966b] W.J. Minkowycz and E.M. Sparrow, Int. J. Heat Mass Transfer, 9 (1966) 1125.

[SUN.2012] H. Sun, G. Lauriat, X. Nicolas, Natural convection and wall condensation or evaporation in humid air filled cavities subjected to wall temperature variations, 2012

[Tan.1991] I. Tanasawa, Advances in condensation heat transfer, Adv. Heat Transfer, Vol. 21, 1991, pp. 55–139.

[Tay.2013] Taylor Oetelaara, Clifton Johnstona, David Wooda, Lisa Hughesc, John Humphreyc, A computational investigation of a room heated by subcutaneous convection—A case study of a replica Roman bath;Energy and Buildings 63 (2013) 59–66

[Teo.2013] Teodosiu R. Integrated moisture (including condensation) – energy – airflow model within enclosures. Experimental validation. *Build. Environ.* 2013;**61**:197-209

[Teo.2014] Raluca Teodosiu, Lidia Niculita, Catalin Teodosiu, Computational Fluid Dynamics Based Modeling of a Linear Heat Source, Enviromental Engineering Management Journal, Vol. 13, No. 8, August 2014

[TEO.2015] Cătălin Teodosiu, Viorel Ilie, and Raluca Teodosiu, Condensation Model for Application of Computational Fluid Dynamics in Buildings, International Journal of Materials, Mechanics and Manufacturing, Vol. 3, No. 2, May 2

[Yad] G. Yadigaroglu Swiss Federal Institute of Technology (ETH), Nuclear Engineering Laboratory, Zurich (CH)COMPUTATIONAL FLUID DYNAMICS FOR NUCLEAR APPLICATIONS: FROM CFD TO MULTI-SCALE CMFD;

[Yiz.2011] DISSERTATION by YIZHOU YAN, DEVELOPMENT OF A COUPLED CFD SYSTEM-CODE CAPABILITY (WITH A MODIFIED POROUS MEDIA MODEL) AND ITS APPLICATIONS TO SIMULATE CURRENT AND NEXT GENERATION REACTORS;Submitted in partial fulfillment of the requirements for the degree of Doctor of Philosophy in Nuclear Engineering in the Graduate College of the University of Illinois at Urbana-Champaign, 2011;

[Wan.2014] Yi Wang, Xiaojing Meng, Xiaoni Yang, Jiaping Liu, Influence of convection and radiation on the thermal environment in an industrial building with buoyancy-driven natural ventilation, Energy and Buildings 75 (2014) 394-401

[Wel.1961] 5. Welch, J. F. and Westwater, J. W., "Microscopic Study of Dropwise Condensation," Proceedings of the Second International Heat Transfer Conference, Vol. II, 1961, pp. 302-309.

[Wen.1936] R.N. Wenzel, Resistance of solid surfaces to wetting by water, Ind Eng. Chem. 28 (8) (1936) 988-994.

[Why.2008] Whyman, G.; Bormashenko, Edward; Stein, Tamir (2008). "The rigirious derivation of Young, Cassie–Baxter and Wenzel equations and the analysis of the contact angle hysteresis phenomenon". Chemical Physics Letters 450 (4–6): 355–359